



National Environmental  
Research Program

TROPICAL ECOSYSTEMS *hub*

**Milestone Report**

Project 11.1 – Building resilient communities for  
Torres Strait futures

## Downscaled Climate Projections for the Torres Strait Region: 8 km<sup>2</sup> results for 2055 and 2090

Jack Katzfey, Wayne Rochester (CSIRO Marine and  
Atmospheric Research)

May 2012



Australian Government

Department of Sustainability, Environment,  
Water, Population and Communities



**NERP Tropical Ecosystems Hub Project 11.1**  
**'Building resilient communities for Torres Strait futures'**

**Downscaled Climate Projections for the Torres Strait Region:**  
**8 km<sup>2</sup> results for 2055 and 2090**

Jack Katzfey, Wayne Rochester (CSIRO Marine and Atmospheric Research)

May 2012

**1. Modelling procedure used to generate the results in this report.**

The section briefly describes the process used to produce the downscaled results presented here. The dynamical downscaling conducted in the Pacific Climate Change Science Program (PCCSP) consisted of a primary set of simulations from which climate projections were derived, as well as a series of additional simulations designed to assess the uncertainty associated with those projections. All primary simulations were completed using CSIRO's global stretched-grid, Conformal Cubic Atmospheric Model (CCAM; McGregor and Dix, 2008) run at 60 km<sup>2</sup> horizontal resolution over the entire globe, while further downscaling to 8 km<sup>2</sup> was conducted for selected partner countries. The CCAM model was chosen for the downscaling because it is a global atmospheric model, so it was possible to bias-adjust the sea-surface temperature in order to improve upon large-scale circulation patterns. In addition, the use of a stretched grid eliminates the problems caused by lateral boundary conditions in limited-area models. The model has been well tested in various model inter-comparisons and in downscaling projects over the Australasian region (Corney et al., 2010).

CCAM 60 km<sup>2</sup> global simulations

These simulations were performed for six host global climate models (CSIRO-Mk3.5, ECHAM/MPI-OM, GFDL-CM2.0, GFDL-CM2.1, MIROC3.2 (medres) and UKMO-HadCM3) that were deemed to have acceptable skill in simulating the climate of the PCCSP region. For these simulations:

- The equivalent CO<sub>2</sub>, direct aerosol effect and ozone distribution for the SRES A2 (high) emissions scenario were used (except in simulating the current climate, which used 20c3m equivalents).
- Monthly, bias-adjusted sea-surface temperature and sea-ice fraction output from the host global climate models was used. Bias adjustment refers to the removal of model errors in the present day, mean state climate. In this case, the sea-surface temperature bias-adjustment was calculated by computing the monthly average biases of the global models for the 1971-2000 period, relative to the observed climatology, based upon the method of Reynolds (1988). These monthly biases were then subtracted from the global climate model monthly sea-surface temperature output throughout the simulation. This approach preserves the inter- and intra-annual variability and the climate change signal of the host global climate models.
- No atmospheric input from the global climate models was used, as the bias-adjusted sea-surface temperature is considered sufficient information to drive CCAM. In addition, the bias-adjustment makes the global climate model atmospheric fields incompatible with the

sea-surface temperature distributions. It is assumed that the fixed, monthly adjustment is appropriate over the entire course of the simulation, which may be a disadvantage of the approach.

- The period 1961-2099 was simulated for the A2 (high) emissions scenario only.

### CCAM 8 km<sup>2</sup> regional simulations

Three global models (GFDL-CM2.1, UKMO-HadCM3 and ECHAM5 60 km CCAM global simulations) were selected for further downscaling to 8 km<sup>2</sup>. Of the six host models, these show a low, middle and high amount of global warming into the future, respectively. Due to the very high demand for computer resources when downscaling at 8 km<sup>2</sup> resolution, the temporal and spatial extent of the simulations was limited. Only the 1980-1999, 2046-2065 and 2080-2099 time periods were simulated for seven 1000 km x 1000 km regions, including Papua New Guinea, East Timor, Fiji, Solomon Islands, Vanuatu, Samoa and the Federated States of Micronesia. The results from the PNG simulation were used in this study because they also cover the Torres Strait region.

## 2. Downscaled projection results

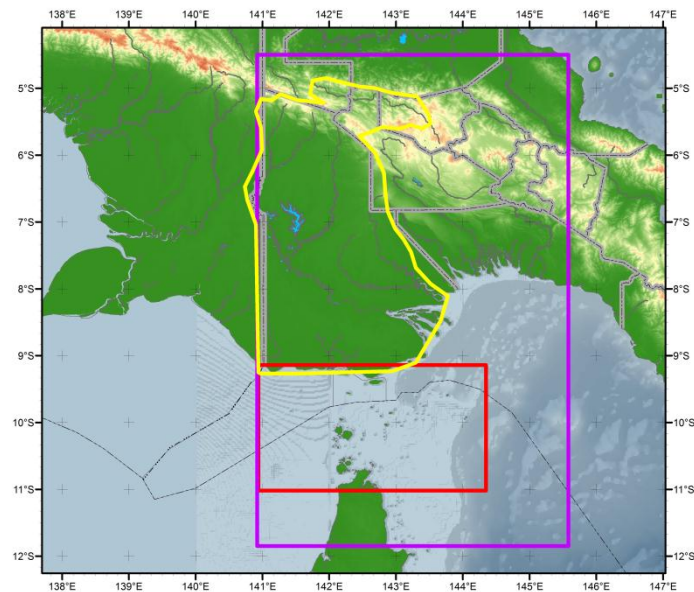


**Figure 1: The Torres Strait Island region (small red box) and Fly River catchment (yellow box) discussed in the text**

The topography of the Torres Strait Island (TSI) and central PNG is shown in Figure 1. Annual means of key variables are presented next, followed by monthly climatology for the TSI region and Fly River catchment (FRC).

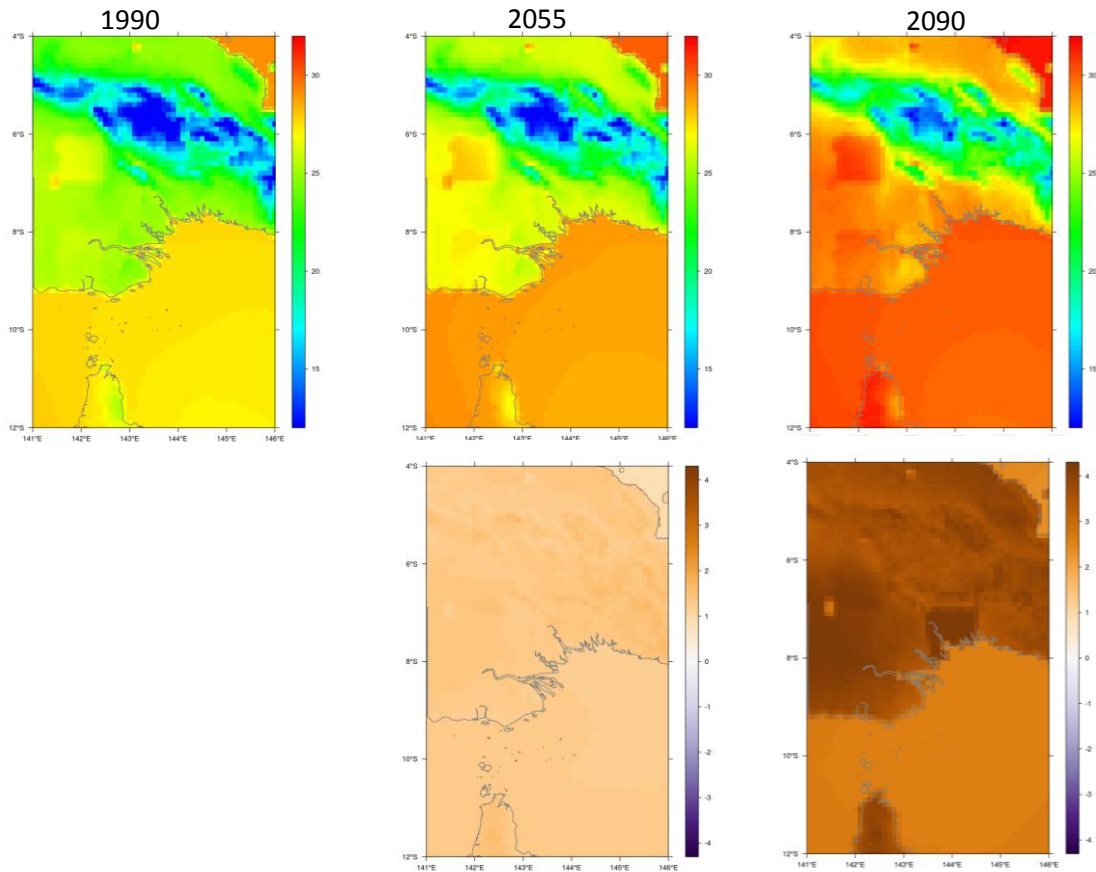
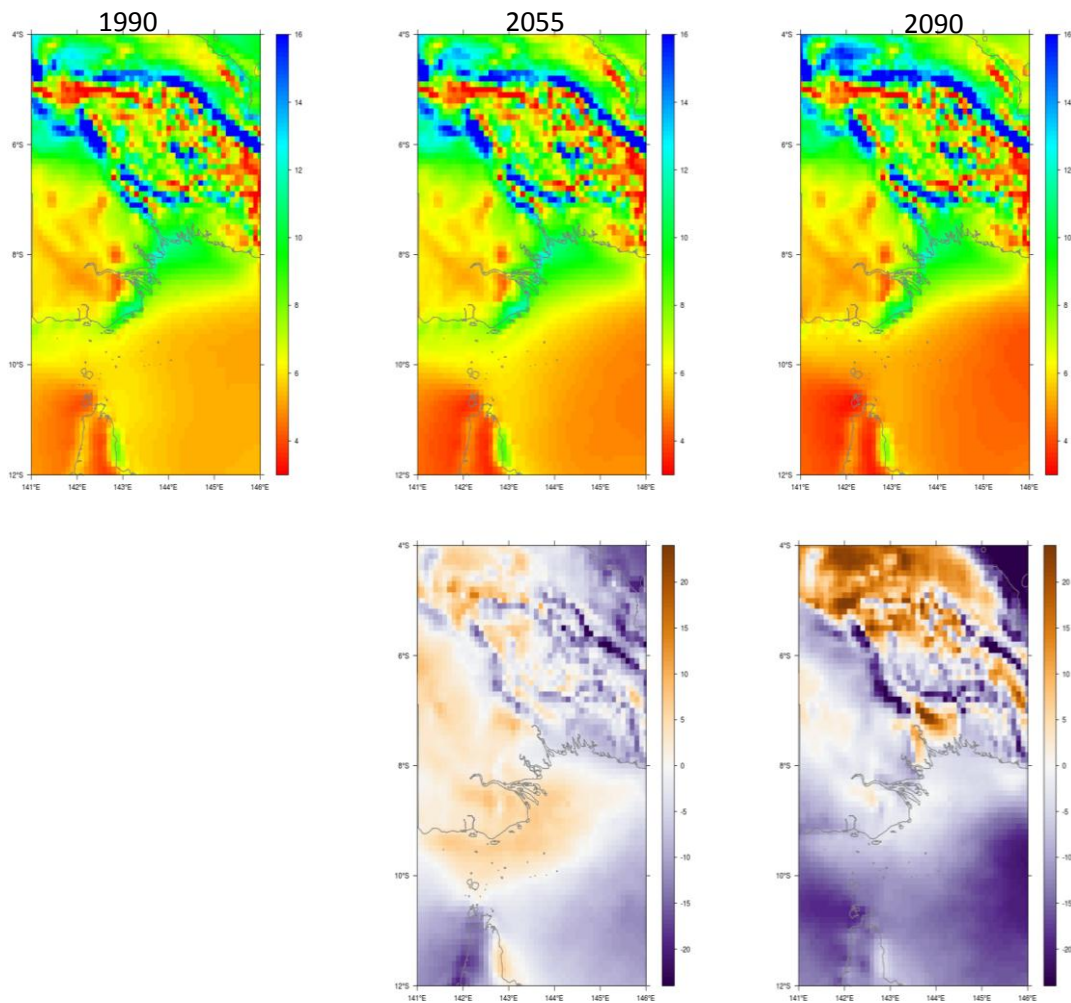


Figure 2: Annual mean surface temperature ( $^{\circ}\text{C}$ , top row) and changes relative to 1990 (bottom row). Left column is for 1990, middle column is for 2055 and right column is for 2090. All plots are for the 3-model mean from the CCAM  $8\text{ km}^2$  simulations.

The plots of annual mean surface temperature over central PNG and the TSI (Figure 2) show the warmer values over the ocean and the coldest values over the higher mountains of PNG. The mean annual surface temperature increases nearly uniformly by  $1\text{-}1.5^{\circ}\text{C}$  by 2055, with slightly lesser increases over the oceans relative to the land. By 2090, the increases over land are around  $2.5^{\circ}\text{C}$  or greater, while over the ocean the increases are less than  $2.5^{\circ}\text{C}$ . Slightly greater warming (nearly  $4^{\circ}\text{C}$ ) is evident over FRC by 2090.

Comparison of these numbers with those produced by Suppiah et al. (2010) (hereafter called S10) based upon 24 global climate model (GCM) outputs show broad similarity. However, by 2055, our warming is slightly higher than their median (50<sup>th</sup> percentile was  $1.48^{\circ}\text{C}$ ) and the range is much reduced due to downscaling only 3 GCMs versus the 24 GCMs used in S10. Similarly, for 2090 the S10 median was  $2.07^{\circ}\text{C}$  versus the current study median of  $2.5^{\circ}\text{C}$ .



**Figure 3: Annual mean rainfall rate ( $\text{mm day}^{-1}$ , top row) and changes relative to 1990 (bottom row). Left column is for 1990, middle column is for 2055 and right column is for 2090. All plots are for the 3-model mean from the CCAM  $8 \text{ km}^2$  simulations.**

The distribution of the annual mean rainfall (Figure 3) shows a complex pattern, with larger rainfall amounts over the slopes of the PNG mountains and along the coastal regions where trade winds flow on land at certain times of the year, triggering rainfall. The veracity of this pattern of rainfall has been checked against the Tropical Rainfall Measuring Mission (TRMM) (not shown). The simulated rainfall pattern shows slightly more rainfall over TSI (around  $6 \text{ mm d}^{-1}$ ) than to the east or west of the islands.

The change in annual rainfall also shows a complex pattern, with decreases in the southern portion of the domain and with large ( $\pm 15\%$ ) changes over the mountains of PNG. The changes over TSI by 2055 are generally small (less than  $5\%$ ), with slight decreases to the south and slight increases in the northern part of the TSI. By 2090, a large decrease in annual rainfall is evident (around  $-10\%$ ) over the TSI region, with greater decreases over western regions ( $-15\%$ ) and further to the east ( $-15\%$ ). Increases of annual rainfall up to around  $20\%$  are evident along the northern shores of PNG as well as along some of the mountain slopes. For the FRC, the annual rainfall changes are generally small.

The future rainfall changes over TSI presented here (little change by 2055 and decreases of -10% by 2090) are different than in S10, where they indicated increases of 2% by 2050 and 3.21% by 2070. It needs to be investigated whether this is a result of the downscaling or due to the small group of models selected.

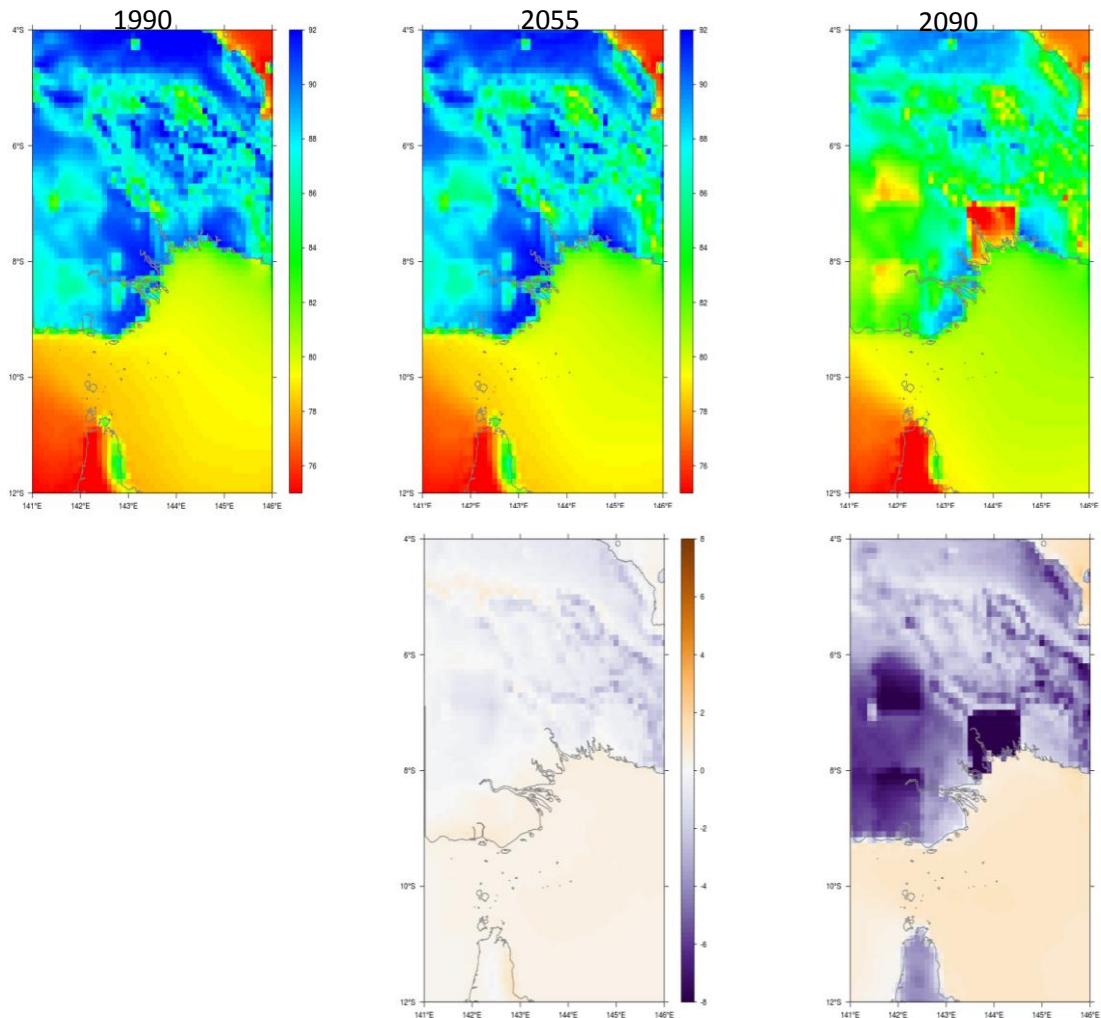


**Figure 4: Annual mean surface relative humidity (%), top row) and changes relative to 1990 (bottom row). Left column is for 1990, middle column is for 2055 and right column is for 2090. All plots are for the 3-model mean from the CCAM 8 km simulations.**

Annual mean surface relative humidity (Figure 4) shows larger values (85-90%) over PNG, related to the cooler and more humid night-time conditions. Variation related to land-use and topography are also evident. Over the oceans, values are less than 80%. Over TSI, relative humidity is around 78%, with a gradient to lower humidity to the west. A sharp gradient in relative humidity is evident across the Cape York Peninsula, with higher values (85%) on the eastern side and lower values on the western side (75%).

By 2055, the relative humidity changes little. However, by 2090 the annual relative humidity shows general decreases over land of more than 5%, primarily related to the increase in temperatures. Over the oceans and TSI, little change in relative humidity is noted. These changes are generally similar to S10, who also indicated little change.

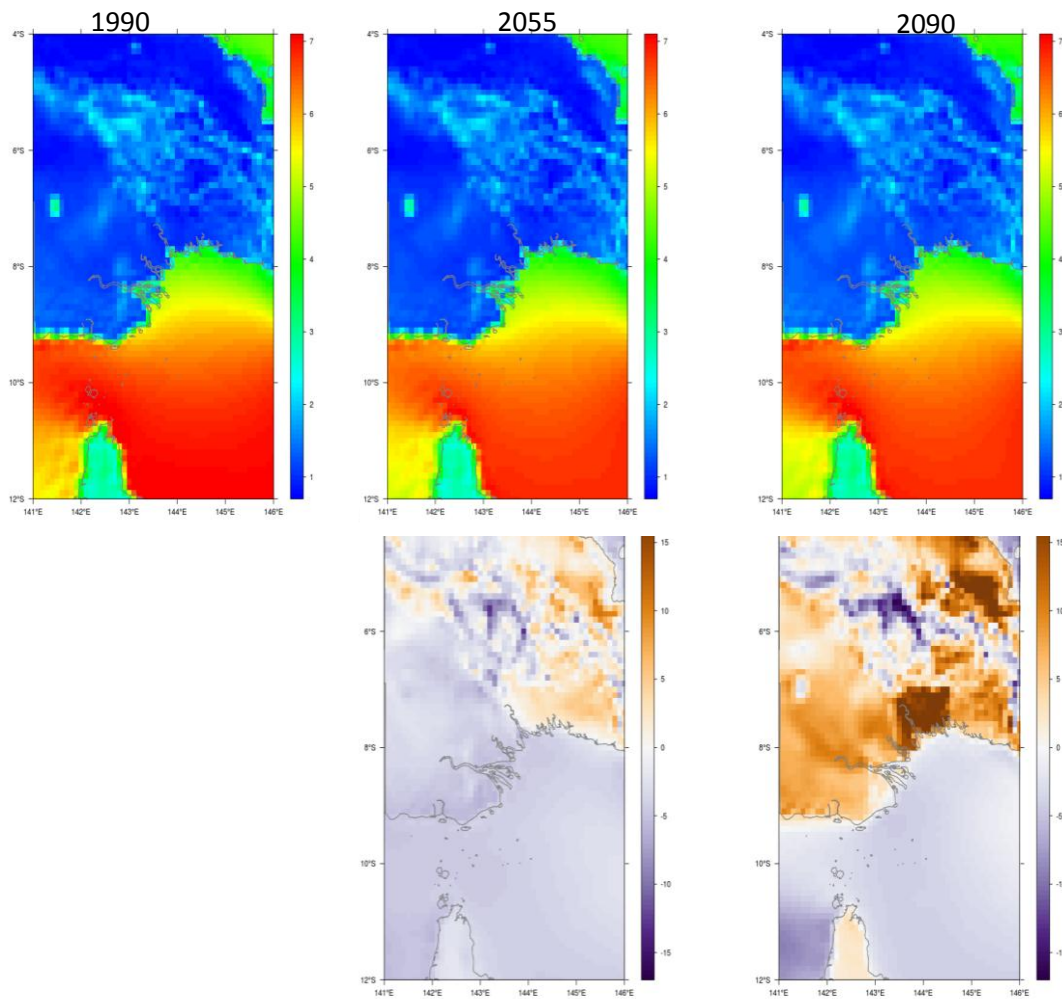


Figure 5: Annual mean 10 m wind speed ( $\text{m s}^{-1}$ , top row) and changes relative to 1990 (bottom row). Left column is for 1990, middle column is for 2055 and right column is for 2090. All plots are for the 3-model mean from the CCAM 8 km simulations.

Annual mean wind speed (Figure 5) shows the expected pattern, with higher speeds over the ocean ( $6\text{--}7 \text{ m s}^{-1}$ ) relative to the land ( $1\text{--}2 \text{ m s}^{-1}$ ), associated with the monsoonal flow over the oceans. This pattern is due to the lower friction of the ocean surface. Slightly higher values of wind speed are also evident on the mountain peaks.

There is little change in wind speeds by 2055 (generally less than 1%). By 2090, the wind speed changes are larger, with slight decreases (less than 5%) over the oceans and TSI, but some increases over the land areas (greater than 10%), except over mountainous regions where decreases are again observed.

S10 indicated slight increases in wind speed: +0.6% by 2050 and + 0.74% by 2090, in contrast to the slight decreases noted here.

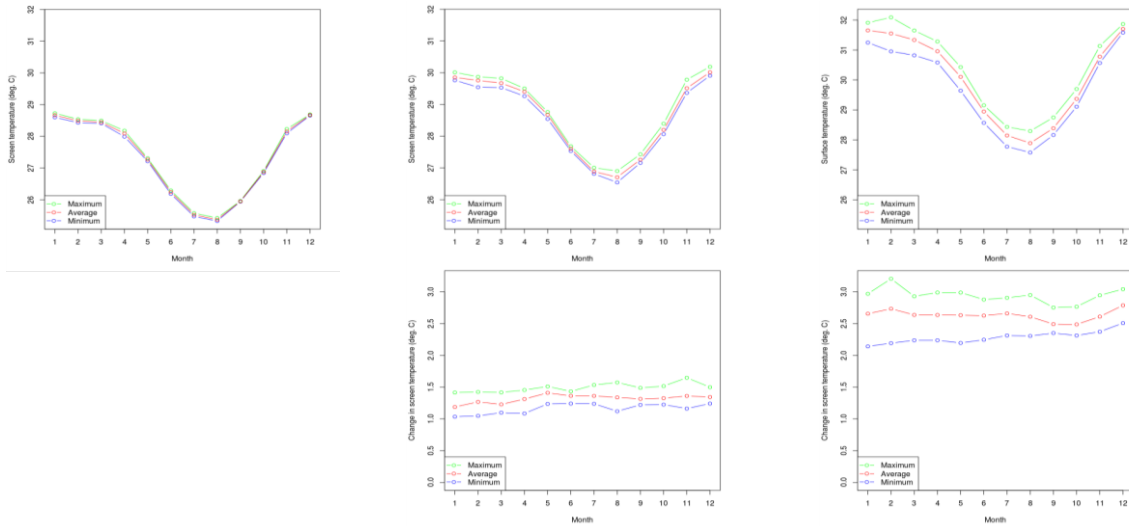


Figure 6: Torres Strait Island region climatology from CCAM 8 km<sup>2</sup> multi-model mean for screen temperature (C) for 1990 (left), 2055 (centre) and 2090 (right). Bottom set of images are the changes from 1990.

The seasonal cycle of surface air temperature (or screen temperature, which is the air temperature at 2 m above surface) for the TSI region is shown in Figure 6. The seasonal cycle shows coolest temperatures in July and August and warmest temperatures in December through March.

By 2055, there is a warming of 1.3<sup>o</sup>C throughout the year, increasing to a warming of 2.6<sup>o</sup>C by 2090. This uniform seasonal warming trend is similar to S10, though the values are about 0.5<sup>o</sup>C greater.

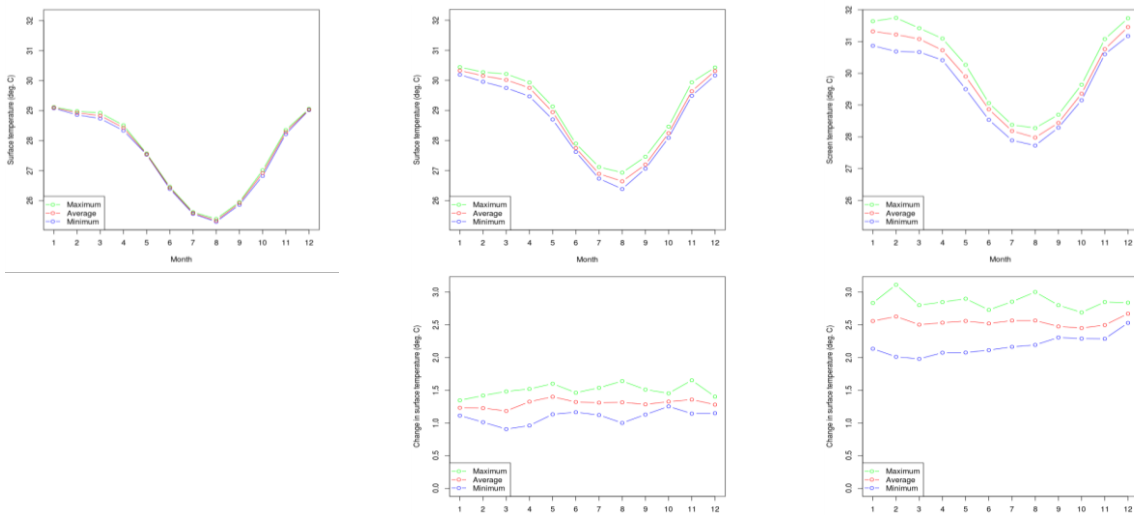


Figure 7: Torres Strait Island region climatology from CCAM 8 km multi-model mean for surface temperature (°C) for 1990 (left), 2055 (centre) and 2090 (right). Bottom set of images are the changes from 1990.

The seasonal cycle of surface temperature for the TSI region is shown in Figure 7. Note that this is very similar to that of the screen temperatures (Figure 6). The seasonal cycle shows coolest temperatures in July and August and warmest temperatures in December through March.

By 2055, there is a warming of 1.0°C throughout the year, increasing to a warming of 2.5°C by 2090.

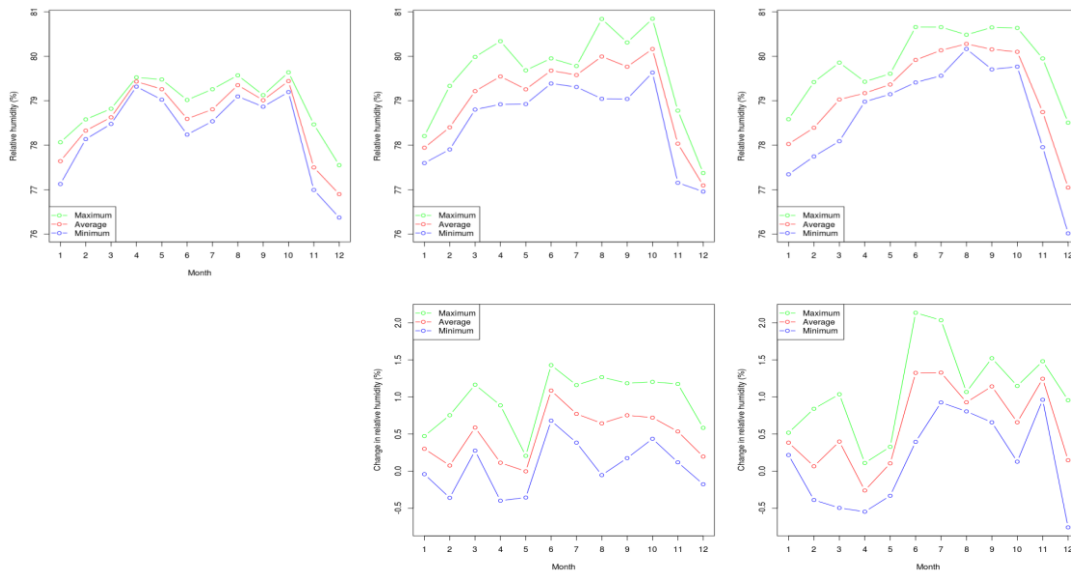
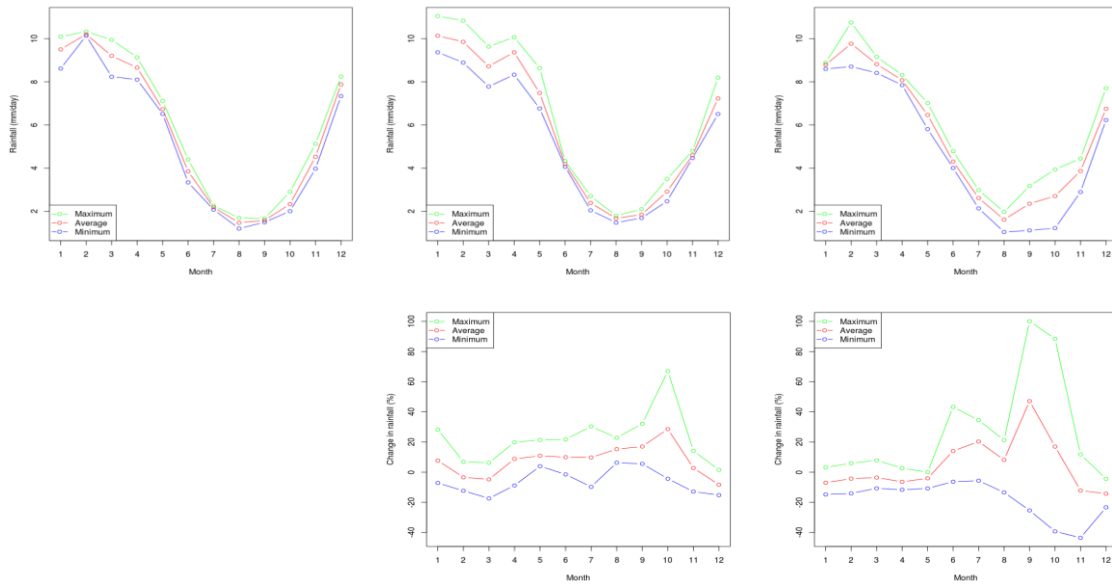


Figure 8: Torres Strait Island region climatology from CCAM 8 km multi-model mean for surface relative humidity (%) for 1990 (left), 2055 (centre) and 2090 (right). Bottom set of images are the changes from 1990.

The annual cycle of surface relative humidity shows little variation over the year for the TSI region, with only slightly lesser values in the November to January period.

As indicated previously in Figure 4, the changes into the future are small, with slight increases of around 0.5% by 2090, especially in the June to November period.

The changes noted in S10 were also small, consistent with our results. However, S10 indicated slight decreases in September to October which contrasts with increases in our results.



**Figure 9: Torres Strait Island region climatology from CCAM 8 km<sup>2</sup> multi-model mean for rainfall (mm day<sup>-1</sup>) for 1990 (left), 2055 (centre) and 2090 (right). Bottom set of images are the percent changes from 1990.**

The rainfall shows an annual cycle with peak values around 8-10 mm d<sup>-1</sup> in January through April and minimum values of around 2 mm d<sup>-1</sup> in August.

Under climate change, the rainfall for this region shows slight increases of around 5%, with greater increases in October of up to 20% by 2055. By 2090, the rainfall shows slight decreases in the first half of the year (around 5%), but with significant increases from June to October of up to 40%.

The changes in rainfall indicated here are larger than those noted in S10. By 2050, S10 indicated a 0.5 to 2.7% increase, which though broadly similar, does not capture the larger increases indicated here, especially in October (nearly 20% increase). By 2090, the rainfall in S10 was projected to increase by around 3-4% except for JJA, where changes of less than 1% were indicated. A much larger increase in rainfall is projected here.

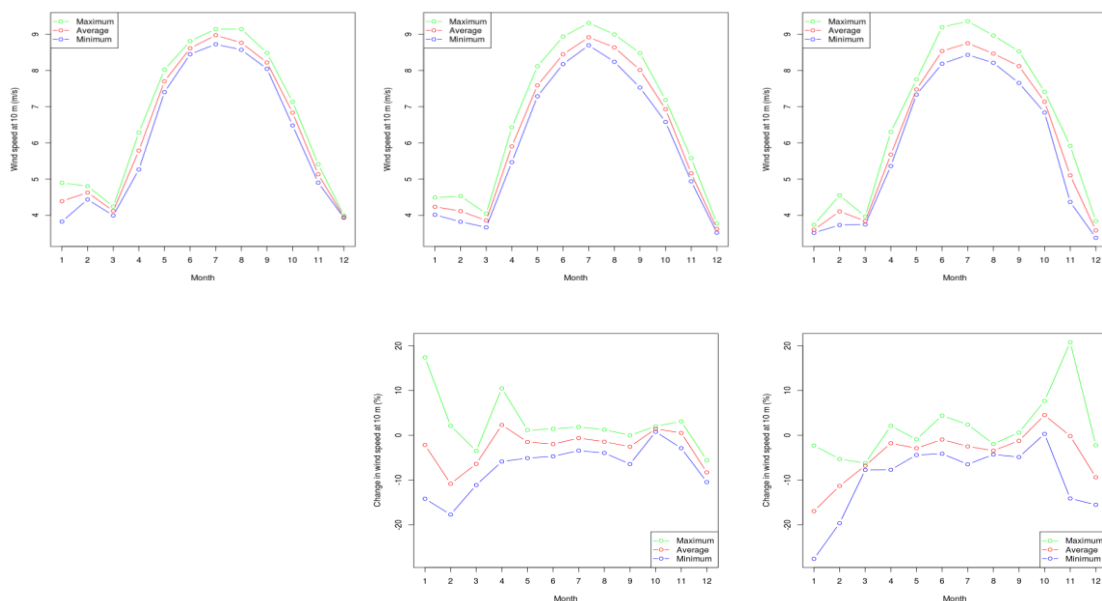


Figure 10: Torres Strait Island region climatology from CCAM 8 km<sup>2</sup> multi-model mean for wind speed (m s<sup>-1</sup>) for 1990 (left), 2055 (centre) and 2090 (right). Bottom set of images are the percent changes from 1990.

The wind speed over the TSI region indicates strong winds (around 9 m s<sup>-1</sup>) in June to August and lighter winds (around 4 m s<sup>-1</sup>) in December through March.

The percentage change in wind speed for this region is generally small, but with larger decreases of 5-10% in February and March as well as December by 2055. By 2090, there are general decreases throughout the year (except October, which shows slight increases.) The decreases by 2090 are greater than at 2055, and approach 20% in January.

In S10, the wind speed was projected to increase by 1-3% for all seasons by 2070. This contrasts with our projected decreases in all seasons, with values of up to nearly 30% in January.

Table 1: Comparison of annual mean change for future projections for Suppiah et al. (GCMs) and this report (8 km<sup>2</sup> downscaled CCAM). Screen temperatures are changes in °C, while other variables are percent changes.

A2 scenario	GCM-2050	8km <sup>2</sup> -2055	GCM-2070	8km <sup>2</sup> -2090
Screen temperature (°C)	1.48	1.32	2.07	2.63
Rainfall (%)	2.14	7.84	3.21	4.56
Screen relative humidity (%)	-0.08	0.48	-0.11	0.62
Wind speed (%)	0.59	-2.63	0.74	-4.41

A summary of the annual changes in S10 and this report are summarised in Table 1. Note that S10 used multiple GCMs (18 to 24 depending upon which variable) while the CCAM 8 km<sup>2</sup> results are from downscaling only 3 GCM to 60 km and then 8 km. Also note the slightly different time periods for the two results, especially the last time period (S10 used 2070 while the CCAM 8 km<sup>2</sup> results are for 2090). The changes are also relative to the respective simulated current climatology.

As noted in the text above, the screen temperature changes are similar in the two datasets. The rainfall changes are of similar sign, but the magnitudes vary. By mid-century, the CCAM 8 km<sup>2</sup>

results show stronger increases, which then become closer to S10 by the end of the century. This is partly because the rainfall increase in mid-year is evident in mid-century, but decreases in the early part of the year do not become prominent until later in the century, balancing some of the increases. The decreases in screen relative humidity in S10 are very small (mainly less than -0.1%), while the increases noted in this report are also small, but slightly larger in magnitude (around +0.5%). The biggest difference is in changes to wind speed, with S10 projecting slight (about +0.5%) increase while this report shows significant decreases (from about -2 to -4%). The cause of these differences needs to be examined further.